HOKKAIDO UNIVERSITY

Title	Improved tunnel magnetoresistance characteristics of magnetic tunnel junctions with a Heusler alloy thin film of Co2MnGe and a MgO tunnel barrier
Author(s)	Hakamata, Shinya; Ishikawa, Takayuki; Marukame, Takao et al.
Citation	Journal of Applied Physics, 101(9), 09J513 https://doi.org/10.1063/1.2713209
Issue Date	2007-05-09
Doc URL	https://hdl.handle.net/2115/50615
Rights	Copyright 2007 American Institute of Physics. This article may be downloaded for personal use only. Any other use requires prior permission of the author and the American Institute of Physics. The following article appeared in J. Appl. Phys. 101, 09J513 (2007) and may be found at https://dx.doi.org/10.1063/1.2713209
Type	journal article
File Information	JAP101_09J513.pdf

Hokkaido University Collection of Scholarly and Academic Papers : HUSCAP

Improved tunnel magnetoresistance characteristics of magnetic tunnel junctions with a Heusler alloy thin film of Co_2MnGe and a MgO tunnel barrier

Shinya Hakamata,[a] Takayuki Ishikawa, Takao Marukame, Ken-ichi Matsuda, Tetsuya Uemura, Masashi Arita, and Masafumi Yamamoto[b]
Division of Electronics for Informatics, Graduate School of Information Science and Technology, Hokkaido University, N14, W9, Kita-ku, Sapporo 060-0814, Japan

(Presented on 11 January 2007; received 31 October 2006; accepted 5 January 2007; published online 9 May 2007)

We fabricated magnetic tunnel junctions (MTJs) with a Co-based full-Heusler alloy thin film of Co_2MnGe (CMG) and a MgO tunnel barrier. The microfabricated MTJs with a Co-rich CMG film showed relatively high tunnel magnetoresistance ratios of 83% at room temperature and 185% at 4.2 K. These values are much higher than those previously obtained for CMG/MgO MTJs with a Co-deficient CMG film. © *2007 American Institute of Physics*. [DOI: 10.1063/1.2713209]

Cobalt-based full-Heusler alloy (Co_2YZ) thin films have recently attracted much interest as highly promising ferromagnetic electrodes for spintronic devices.[1–7] This is because of the half-metallic ferromagnetic nature[8] theoretically predicted for some of these alloys[9,10] and because of their high Curie temperatures, which are well above room temperature (RT).[11,12] Relatively high tunnel magnetoresistance (TMR) ratios have been demonstrated at RT for magnetic tunnel junctions (MTJs) with a Co_2YZ thin film.[13–23] We developed fully epitaxial MTJs with a Co_2YZ thin film and a MgO tunnel barrier,[16–19,22–24] and showed a relatively high TMR ratio of 109% at RT (317% at 4.2 K) for $Co_2Cr_{0.6}Fe_{0.4}Al/MgO/Co_{50}Fe_{50}$ MTJs,[23] and a TMR ratio of 90% at RT (192% at 4.2 K) for Co_2MnSi (CMS)$/MgO/Co_{50}Fe_{50}$ MTJs (CMS-MTJs).[22] Compared with these MTJs, previously reported fully epitaxial Co_2MnGe (CMG)$/MgO/Co_{50}Fe_{50}$ MTJs (CMG-MTJs) showed a much lower TMR ratio of 14% at RT (70% at 7 K).[17,18] The CMG film used in the previous study was a Co-deficient CMG film (the film composition was $Co_2Mn_{1.05}Ge_{1.17}$),[17,18] while the CMS film used in the previous study was a Co-rich CMS film (the film composition was $Co_2Mn_{0.84}Si_{0.80}$).[22] Hereafter, we refer to this Co-deficient CMG film as the CMG_d film. Our purpose in the present study was to improve the TMR characteristics of CMG-MTJs. For this purpose, we fabricated CMG-MTJs with a Co-rich CMG film and investigated their TMR characteristics.

We fabricated epitaxial MTJs that consisted of a CMG thin film and a wedge-shaped MgO tunnel barrier. The composition of the CMG film used in this study was determined to be $Co_2Mn_{0.74}Ge_{0.43}$ (Co-rich CMG), with an accuracy of 2%–3% for each element, through inductively coupled plasma analysis. This Co-rich film composition was obtained by using a sputtering target with a composition of $Co_{2.0}Mn_{1.0}Ge_{1.0}$. Hereafter, we refer to this Co-rich CMG film as the CMG_r film. The fabricated epitaxial MTJ layer structure (from the substrate side) consisted of a MgO buffer layer (10 nm), a CMG lower electrode (50 nm), a MgO tunnel barrier (1.6–2.8 nm), a $Co_{50}Fe_{50}$ upper electrode (3 nm), a layer of Ru (0.8 nm), a layer of $Co_{90}Fe_{10}$ (2 nm), a layer of IrMn (10 nm), and a Ru cap (5 nm); this structure was grown on a MgO(001) substrate. Each layer in the MTJ layer structure was successively deposited in an ultrahigh vacuum chamber (with a base pressure of around 6×10^{-8} Pa) through the combined use of magnetron sputtering and electron beam (EB) evaporation. The CMG layer was deposited at RT using magnetron sputtering and subsequently annealed *in situ* at 500–600 °C for 15 min. The MgO tunnel barrier was deposited by EB evaporation at RT. The pressure during the deposition of the MgO tunnel barrier was around 6×10^{-7} Pa. The nominal thickness of the MgO tunnel barrier (t_{MgO}) was varied from 1.6 to 2.8 nm on each 20×20 mm^2 substrate by using a linearly moving shutter during fabrication. All the layers in the MTJ layer structure were deposited with a magnetic field applied. We fabricated MTJs with the layer structure described above by using photolithography and Ar ion milling. The fabricated junction sizes were from 8×8 to 10×10 μm^2. The magnetoresistance was measured with a magnetic field applied along the [110] axis of the Co_2YZ at temperatures from 4.2 K to RT using a dc four-probe method. We defined the TMR ratio as $(RA_{AP}-RA_P)/RA_P$, where RA_{AP} and RA_P are the respective resistance-area products for the antiparallel and parallel magnetization configurations between the upper and lower electrodes. As shown below, as-fabricated (i.e., not *ex situ* annealed) MTJs showed exchange-biased TMR characteristics. Transport properties of as-fabricated MTJs are described below.

X-ray pole figure scans of a CMG_r film deposited at RT and subsequently annealed at 600 °C showed fourfold symmetry of the CMG (111) peaks at $\chi=54.7°$, which gives direct evidence that the 600 °C annealed film is epitaxial and crystallized in the $L2_1$ structure. Because the φ values for the CMG (111) peaks were shifted by 45° with respect to those of the MgO (111) peaks, the crystallographic relationship was CMG (001)[100] ∥ MgO (001)[110] on a 45° in-plane rotation. These structural properties are similar to those previously observed for the CMG_d films.[6,17]

[a]Electronic mail: hakamata@nsed.ist.hokudai.ac.jp
[b]Author to whom correspondence should be addressed; electronic mail: yamamoto@nano.ist.hokudai.ac.jp

 © 2007 American Institute of Physics

Downloaded 15 Nov 2012 to 133.87.26.103. Redistribution subject to AIP license or copyright; see http://jap.aip.org/about/rights_and_permissions

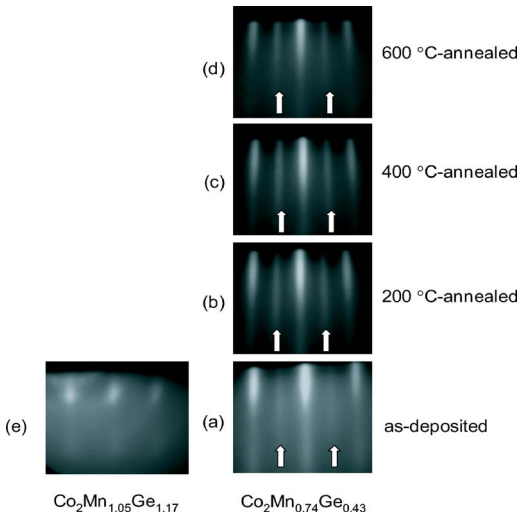


FIG. 1. [(a)–(d)] RHEED patterns, along the azimuth of $[100]_{MgO}$ corresponding to $[110]_{CMG}$, obtained *in situ* for a Co-rich Co_2MnGe (CMG) film during fabrication. The CMG film was deposited at RT on a MgO buffer layer (10 nm) and subsequently *in situ* annealed step by step at 200–600 °C. The substrate was a MgO (001) single crystal. The arrows indicate streak patterns corresponding to CMG (11^*) reflection. (e) A RHEED pattern for comparison, along the azimuth of $[100]_{MgO}$ corresponding to $[110]_{CMG}$, obtained previously for an as-deposited Co-deficient CMG film during fabrication (Ref. 17). Streak patterns corresponding to the CMG (11^*) reflection were not observed.

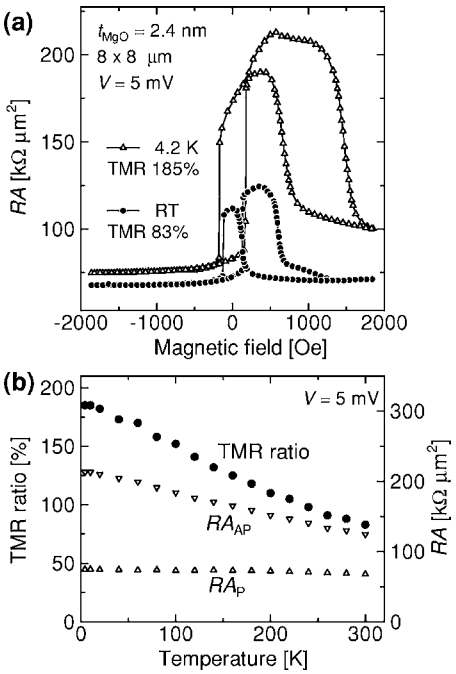


FIG. 2. (a) Typical magnetoresistance curves at a bias voltage (V) of 5 mV at RT and 4.2 K for a fabricated Co_2MnGe (CMG)/MgO/$Co_{50}Fe_{50}$ MTJ with a Co-rich CMG film where the CMG lower electrode was *in situ* annealed at 600 °C after deposition (t_{MgO}=2.4 nm). The junction size was 8×8 μm^2. TMR ratios were 83% at RT and 185% at 4.2 K. (b) TMR ratio, as well as RA_{AP} and RA_P, at V=5 mV for the same MTJ shown in Fig. 2(a) as a function of temperature from 4.2 K to RT, where RA_{AP} and RA_P are the respective resistance-area products for the antiparallel and parallel magnetization configurations between the upper and lower electrodes.

We observed the surface morphologies of the 45-nm-thick CMG_r films deposited on MgO buffer layers (10 nm) using atomic force microscopy. The root mean square (rms) values of the surface roughness increased with postdeposition annealing, from a rms roughness of 0.16 nm for the as-deposited film to 0.41 nm for the 600 °C annealed film. This dependence on postdeposition annealing temperature was in contrast to that previously observed for the CMG_d film, i.e., the rms values of the surface roughness decreased with postdeposition annealing, from a rms value of roughness of 0.40 nm for the as-deposited film to 0.26 nm for the 600 °C annealed film.[6,17]

Figure 1 shows reflection high-energy electron diffraction (RHEED) patterns, along the azimuth of $[100]_{MgO}$ corresponding to $[110]_{CMG}$, observed *in situ* for a CMG_r film deposited at RT on a MgO buffer layer (10 nm) and subsequently annealed *in situ* step by step at 200–600 °C; Fig. 1(e) shows a RHEED pattern obtained previously for an as-deposited CMG_d film for comparison. We did not observe the streak pattern corresponding to the (11^*) reflection for the as-deposited CMG_d film as shown in Fig. 1(e), although we observed streaks corresponding to the (11^*) reflection for the CMG_d film annealed at 600 °C. It is notable that we see streak patterns that correspond to the (11^*) reflection even for the as-deposited CMG_r film [Fig. 1(a)]. The streaks that correspond to the (11^*) reflection for the CMG_r film annealed at 200–600 °C [Figs. 1(b)–1(d)] became sharper and more distinct than those of the as-deposited film [Fig. 1(a)]. The streaks of the (11^*) reflection for the as-deposited film indicate the existence of the $L2_1$ structure even in the as-deposited CMG_r films, which means that the structural properties of the CMG_r films were better than those of the CMG_d films with respect to the degree of structural order.

Next, we will describe the spin-dependent tunneling characteristics of fabricated epitaxial MTJs. Figure 2(a) shows typical magnetoresistance curves at a bias voltage (V) of 5 mV at RT and 4.2 K for an as-fabricated CMG_r/MgO/$Co_{50}Fe_{50}$ MTJ, having a 2.4-nm-thick MgO tunnel barrier, where the lower CMG electrode was *in situ* annealed at 600 °C after deposition. The junction size was 8×8 μm^2. Exchange-biased TMR characteristics were obtained with relatively high TMR ratios of 83% at RT and 185% at 4.2 K. These values are comparable to the TMR ratios of 90% at RT and 192% at 4.2 K previously obtained for CMS/MgO/$Co_{50}Fe_{50}$ MTJs with a Co-rich CMS film, of which the film composition was $Co_2Mn_{0.84}Si_{0.80}$ (Ref. 22); these are significantly enhanced from the lower TMR ratios of 14% at RT and 70% at 7 K previously obtained for CMG/MgO/$Co_{50}Fe_{50}$ MTJs with a Co-deficient CMG film, of which the film composition was $Co_2Mn_{1.05}Ge_{1.17}$.[17,18]

Figure 2(b) plots the TMR ratio, as well as RA_{AP} and RA_P, at V=5 mV for the same MTJ shown in Fig. 2(a) as a function of temperature (T) from 4.2 K to RT. As T decreased from RT to 4.2 K, the TMR ratio increased by a factor of 2.2. If we use parameter $\gamma=\alpha(4.2\ \mathrm{K})/\alpha(\mathrm{RT})$, where α is the TMR ratio, to represent the degree of T dependence of the TMR ratio, γ for CMG_r/MgO/$Co_{50}Fe_{50}$ MTJs was 2.2. This value is comparable to the previously obtained γ =2.1 for CMS/MgO/$Co_{50}Fe_{50}$ MTJs (a TMR ratio of 192% at 4.2 K and 90% at RT)[22] and significantly lower than γ =5.0, which was previously obtained for CMG_d/MgO/$Co_{50}Fe_{50}$ MTJs (a TMR ratio of 70% at 7 K

Downloaded 15 Nov 2012 to 133.87.26.103. Redistribution subject to AIP license or copyright; see http://jap.aip.org/about/rights_and_permissions

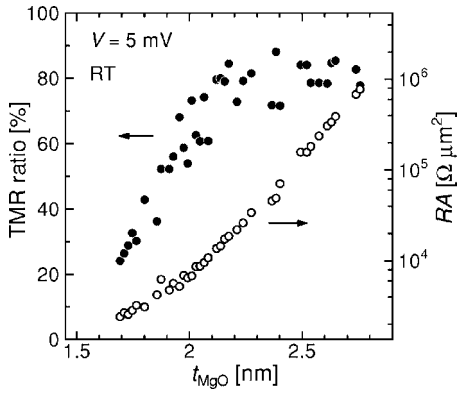


FIG. 3. RA_P and TMR ratio at RT (measured at $V=5$ mV) as a function of MgO tunnel barrier thickness t_{MgO} for fabricated Co_2MnGe (CMG)/MgO/$Co_{50}Fe_{50}$ MTJs with a Co-rich CMG film where the CMG lower electrode was *in situ* annealed at 500 °C after deposition. RA_P represents the resistance-area product *RA* for the parallel magnetization configuration. The junction size was 10×10 μm^2. The scale of the vertical axis for RA_P is logarithmic.

and 14% at RT).[17,18] As shown in Fig. 2(b), RA_{AP} also increased with decreasing *T*, while RA_P was almost independent of *T*. These behaviors were similar to those previously observed for CCFA/MgO/$Co_{50}Fe_{50}$ MTJs (Ref. 24) and CMS/MgO/$Co_{50}Fe_{50}$ MTJs.[22] These behaviors were also observed for $Co_{70}Fe_{30}$/MgO/$Co_{84}Fe_{16}$ MTJs.[25]

Figure 3 plots RA_P and the TMR ratio at RT (measured at $V=5$ mV) as a function of t_{MgO} for the fabricated CMG_r/MgO/$Co_{50}Fe_{50}$ MTJs where the CMG lower electrode was *in situ* annealed at 500 °C after deposition. The junction size was 10×10 μm^2. A clear exponential dependence of R_{AP} on t_{MgO} was observed for the t_{MgO} range of 2.0–2.8 nm, indicating typical tunnel junction behavior. Relatively high TMR ratios from 72% to 88% were obtained at RT for this wide range of t_{MgO} from (2.0–2.8 nm).

We estimated the spin polarization for the CMG_r electrodes by using Jullière's model for the TMR ratio;[26] TMR $=2P_1P_2/(1-P_1P_2)$, where P_1 and P_2 are the spin polarizations at the Fermi level (E_F) of the ferromagnetic electrodes in MTJs. We first estimated the effective spin polarization for the $Co_{50}Fe_{50}$ electrode from the TMR ratio of 146% at 4.2 K (96% at RT) obtained for the identically fabricated epitaxial $Co_{50}Fe_{50}$/MgO/$Co_{50}Fe_{50}$ MTJs by using Jullière's model. Thus, the effective spin polarization value obtained for the $Co_{50}Fe_{50}$ electrode (P_{CoFe}) was 0.65 at 4.2 K (0.57 at RT). Then, we estimated the effective spin polarization of the CMG film (P_{CMG}) from the TMR ratio of 185% at 4.2 K (83% at RT) for the epitaxial CMG_r/MgO/$Co_{50}Fe_{50}$ MTJs by using Jullière's model with P_{CoFe} of 0.65 at 4.2 K (0.57 at RT). The obtained effective spin polarization or tunneling spin polarization values of P_{CMG} were 0.74 at 4.2 K and 0.51 at RT. These P_{CMG} values are comparable to previously obtained values of 0.75 at 4.2 K and 0.54 at RT for the CMS films.[22]

The enhanced TMR ratios for the CMG/MgO/$Co_{50}Fe_{50}$ MTJs fabricated with a Co-rich CMG film demonstrated that the lower TMR ratios observed previously for the CMG/MgO/$Co_{50}Fe_{50}$ MTJs with a Co-deficient CMG film[17,18] were not due to an intrinsic property of the Co-based full-Heusler alloy of Co_2MnGe. The improved TMR characteristics in terms of the TMR ratio or the effective spin polarization at E_F are probably related to the improved structural properties of the CMG film in terms of the degree of structural order.

In summary, we fabricated epitaxial MTJs with a Co-based full-Heusler alloy thin film of CMG and a MgO tunnel barrier. The microfabricated MTJs with a Co-rich CMG film demonstrated relatively high tunnel magnetoresistance ratios of 83% at RT and 185% at 4.2 K. These values are much higher than those previously obtained for CMG/MgO/$Co_{50}Fe_{50}$ MTJs with a Co-deficient CMG film.

This work was partly supported by a Grant-in-Aid for Scientific Research (B) (Grant No. 18360143), a Grant-in-Aid for Creative Scientific Research (Grant No. 14GS0301), and a Grant-in-Aid for Young Scientists (B) (Grant No. 17760267) from the Ministry of Education, Culture, Sports, Science and Technology, Japan.

[1] T. Ambrose, J. J. Krebs, and G. A. Prinz, Appl. Phys. Lett. **76**, 3280 (2000).
[2] I. Galanakis, P. H. Dederichs, and N. Papanikolaou, Phys. Rev. B **66**, 174429 (2002).
[3] X. Y. Dong *et al.*, Appl. Phys. Lett. **86**, 102107 (2005).
[4] S. Wurmehl *et al.*, J. Phys. D **39**, 803 (2006).
[5] K.-i. Matsuda, T. Kasahara, T. Marukame, T. Uemura, and M. Yamamoto, J. Cryst. Growth **286**, 389 (2006).
[6] T. Ishikawa, T. Marukame, K.-i. Matsuda, T. Uemura, M. Arita, and M. Yamamoto, J. Appl. Phys. **99**, 08J110 (2006).
[7] H. Kijima, T. Ishikawa, T. Marukame, H. Koyama, K. Matsuda, T. Uemura, and M. Yamamoto, IEEE Trans. Magn. **42**, 2688 (2006).
[8] R. A. de Groot, F. M. Mueller, P. G. van Engen, and K. H. J. Buschow, Phys. Rev. Lett. **50**, 2024 (1983).
[9] S. Ishida, S. Fujii, S. Kashiwagi, and S. Asano, J. Phys. Soc. Jpn. **64**, 2152 (1995).
[10] S. Picozzi, A. Continenza, and A. J. Freeman, Phys. Rev. B **66**, 094421 (2002).
[11] P. J. Webster, J. Phys. Chem. Solids **32**, 1221 (1971).
[12] T. Block, C. Felser, G. Jakob, J. Ensling, B. Mühling, P. Gütlich, and R. J. Cava, J. Solid State Chem. **176**, 646 (2003).
[13] K. Inomata, S. Okamura, R. Goto, and N. Tezuka, Jpn. J. Appl. Phys., Part 2 **42**, L419 (2003).
[14] S. Kämmerer, A. Thomas, A. Hütten, and G. Reiss, Appl. Phys. Lett. **85**, 79 (2004).
[15] H. Kubota, J. Nakata, M. Oogane, Y. Ando, A. Sakuma, and T. Miyazaki, Jpn. J. Appl. Phys., Part 2 **43**, L984 (2004).
[16] T. Marukame, T. Kasahara, K.-i. Matsuda, T. Uemura, and M. Yamamoto, Jpn. J. Appl. Phys., Part 2 **44**, L521 (2005).
[17] M. Yamamoto, T. Marukame, T. Ishikawa, K.-i. Matsuda, T. Uemura, and M. Arita, J. Phys. D **39**, 824 (2006).
[18] T. Marukame, T. Ishikawa, K.-i. Matsuda, T. Uemura, and M. Yamamoto, J. Appl. Phys. **99**, 08A904 (2006).
[19] T. Marukame, T. Ishikawa, K.-i. Matsuda, T. Uemura, and M. Yamamoto, Appl. Phys. Lett. **88**, 262503 (2006).
[20] Y. Sakuraba, M. Hattori, M. Oogane, Y. Ando, H. Kato, A. Sakuma, T. Miyazaki, and H. Kubota, Appl. Phys. Lett. **88**, 192508 (2006).
[21] N. Tezuka, N. Ikeda, S. Sugimoto, and K. Inomata, Appl. Phys. Lett. **89**, 252508 (2006).
[22] T. Ishikawa, T. Marukame, H. Kijima, K.-i. Matsuda, T. Uemura, M. Arita, and M. Yamamoto, Appl. Phys. Lett. **89**, 192505 (2006).
[23] T. Marukame, T. Ishikawa, S. Hakamata, K.-i. Matsuda, T. Uemura, and M. Yamamoto, Appl. Phys. Lett. **90**, 012508 (2007).
[24] T. Ishikawa, T. Marukame, S. Hakamata, K.-i. Matsuda, T. Uemura, and M. Yamamoto, J. Magn. Magn. Mater. **310**, 1897 (2007).
[25] S. S. P. Parkin, C. Kaiser, A. Panchula, P. M. Rice, B. Hughes, M. Samant, and S.-H. Yang, Nat. Mater. **3**, 862 (2004).
[26] M. Jullière, Phys. Lett. **54A**, 225 (1975).

Downloaded 15 Nov 2012 to 133.87.26.103. Redistribution subject to AIP license or copyright; see http://jap.aip.org/about/rights_and_permissions